Crystalline electric fields and the magnetic ground state of the Heusler intermetallic $YbRh_2Pb$

D. A. Sokolov,[1,*] M. S. Kim,[1] M. C. Aronson,[1] C. Henderson,[2] and P. W. Stephens[3]
[1]*Department of Physics, The University of Michigan, Ann Arbor, Michigan 48109-1120, USA*
[2]*Department of Geological Sciences, The University of Michigan, Ann Arbor, Michigan 48109-1120, USA*
[3]*Department of Physics and Astronomy, State University of New York, Stony Brook, New York 11794, USA*
(Received 28 March 2007; revised manuscript received 17 March 2008; published 1 May 2008)

We have synthesized an intermetallic compound with a distorted Heusler structure, $YbRh_2Pb$. We present a study of the magnetic, thermal, and transport properties. Heat capacity measurements revealed that $YbRh_2Pb$ magnetically orders below $T_N=0.57$ K from a paramagnetic state with substantial crystal electric field splitting. Magnetic field further splits the ground state, which leads to the suppression of magnetic order in $YbRh_2Pb$.

DOI: 10.1103/PhysRevB.77.174401 PACS number(s): 75.40.Cx, 71.20.Eh

I. INTRODUCTION

Analysis of the magnetic properties of compounds containing rare earths is complicated when the Kondo temperature and the crystalline electric field (CEF) splitting of the ground state are comparable to the ordering temperature. The CEF reduces the degeneracy of the total angular momentum J, often leading to deviations from the Curie–Weiss behavior of the temperature dependent magnetic susceptibility. The CEF scheme in high symmetry crystal structures can be established by using heat capacity and magnetic susceptibility measurements, making it straightforward in this case to isolate possible Kondo effects as well as phenomena related to the magnetic ordering. The Heusler compounds are an especially attractive class of materials in which to pursue such studies, as they contain a cubic lattice of rare-earth ions.[1] Rare-earth based Heusler compounds generally order antiferromagnetically at low temperatures due to the conduction electron mediated Ruderman–Kittel–Kasuya–Yosida (RKKY) interaction among well-localized rare earth moments.[2–10] Intriguingly, coexistence of antiferromagnetism and superconductivity was reported for some of these compounds.[2,4,5,7–9] In this paper, we report a Yb-based tetragonally distorted Heusler compound, $YbRh_2Pb$, with a magnetic ordering temperature comparable to the splitting in the ground state manifold. The tetragonal distortion of the cubic Heusler structures was previously reported and was attributed to an electronic instability of the band Jahn–Teller type.[11] We demonstrate that the degeneracy of the manifold in $YbRh_2Pb$ is partially lifted by both the CEF and the magnetic field. The magnetism of $YbRh_2Pb$, which is characterized by total angular momentum J, is suppressed by the reduced degeneracy of the ground state.

II. EXPERIMENTAL DETAILS

Samples of $YbRh_2Pb$ were grown from Pb flux. They had the appearance of faceted cubes with a typical dimension of 2 mm. The grains were etched to remove excess Pb by using a 1:1 solution of H_2O_2 and acetic acid. A small amount of one grain was crushed, and a powder x-ray diffraction pattern was collected at room temperature. A Si(111) double crystal monochromator selected a beam of 0.70050(2) Å x rays at the X16C beamline of the National Synchrotron Light Source at Brookhaven National Laboratory. The diffracted x rays were analyzed by using a Ge(111) crystal and detected with a NaI scintillation counter. The sample, on a quartz zero-background holder, was oscillated 2° at each point during data collection. Microanalysis measurements were performed on a CAMECA SX100 electron microprobe at the University of Michigan. The electron beam voltage was 20 keV, the beam current was 10 nA, and the Yb $L\alpha$, Rh $L\alpha$, and Pb $M\alpha$ x-ray intensities were calibrated from synthetic $YbPO_4$, synthetic CeRhSn, and natural PbS standards, respectively. Matrix elements were calculated by using the CAMECA PAP data reduction routine. The magnetization and magnetic susceptibility were measured at temperatures from 1.8 to 300 K by using a superconducting quantum interference device magnetometer and from 300 to 1000 K by using a vibrating sample magnetometer (VSM) from Quantum Design. Measurements of the electrical resistivity and heat capacity were performed by using a Quantum Design physical property measurement system at temperatures from 0.35 to 300 K and in magnetic fields up to 4 T.

III. RESULTS AND DISCUSSION

The electron microprobe experiments found that the stoichiometry was uniform over the surface of the samples, with the elemental ratios for Yb:Rh:Pb of $1\pm0.02:2\pm0.04:1\pm0.02$. Examination of several small grains chipped from the faceted as-grown samples with a Bruker Smart charged-coupled device X-ray diffractometer revealed that they were multiply twinned. The powder x-ray diffraction pattern was indexed and refined by using TOPAS software.[12] The powder x-ray diffraction pattern showed the presence of Pb and several other weak unidentified peaks. The unit cell was found to be tetragonal, with dimensions of $a=4.5235(4)$ Å, $c=6.9864(6)$ Å, and a probable space group of $I4/mmm$. The small, high symmetry unit cell suggested a distorted Heusler alloy structure, and indeed, a satisfactory refinement was found with Yb at (0,0,0), Pb at (0,0,1/2), and Rh at (0,1/2,1/4). Refinement of occupancies showed no significant mixing of atoms in the various sites (less than 5%). The crystal structure of $YbRh_2Pb$ is shown in Fig. 1. The observation of cube-shaped grains containing

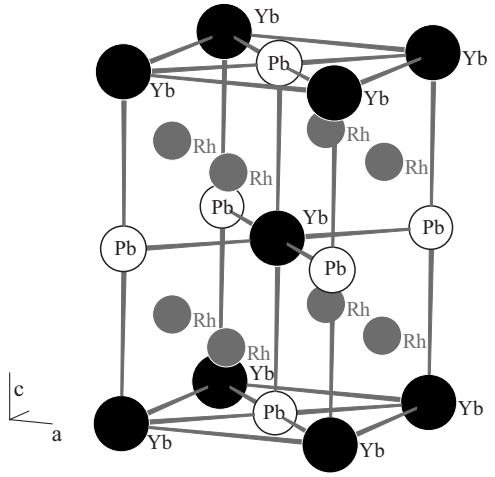

FIG. 1. Crystal structure of $YbRh_2Pb$. Rh atoms occupy (0,1/2,1/4) sites, Yb atoms are at (0,0,0), and Pb atoms are at (0,0,1/2) positions.

multiple twins suggested that the sample material was a cubic phase when it solidified from the melt and transformed into the tetragonal phase when it cooled. A similar behavior in Heusler intermetallic phases was previously noted and ascribed to an electronic band-driven Jahn–Teller distortion.[11]

The electrical resistivity ρ was measured from 0.35 to 300 K. As shown in Fig. 2, the resistivity is that of a good metal, decreasing from the value of 16 $\mu\Omega$ cm at 300 K to 2 $\mu\Omega$ cm at the lowest temperature. The inset of Fig. 2 shows a partial superconducting transition at $T_c=7.2$ K due to residual Pb flux, followed by another partial superconducting transition at $T_c=3$ K, which we believe is due to trace amounts of superconducting $RhPb_2$.[13] We performed Meissner effect measurements, which confirmed these conclusions, finding a volume fraction of less than 1% for the proposed Pb inclusions and an even smaller volume fraction for $RhPb_2$. The almost linear temperature dependence of $\rho(T)$ demonstrated in Fig. 2 for temperatures above ~70 K is remarkable. While this linearity is manifestly not that of a normal Fermi liquid ground state, it may indicate that the

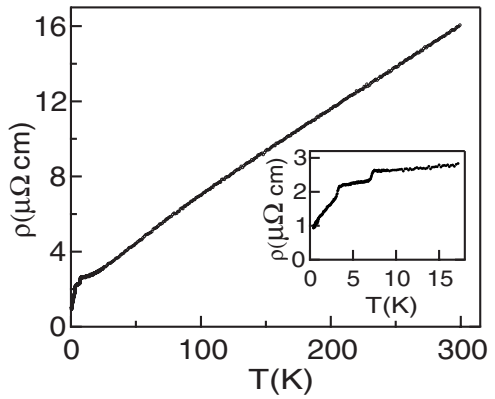

FIG. 2. Temperature dependence of the electrical resistivity of $YbRh_2Pb$ measured in zero field. Inset: Expanded view of low temperatures, showing two partial superconducting transitions at 7.2 and 3 K due to trace amounts of Pb and $RhPb_2$, respectively.

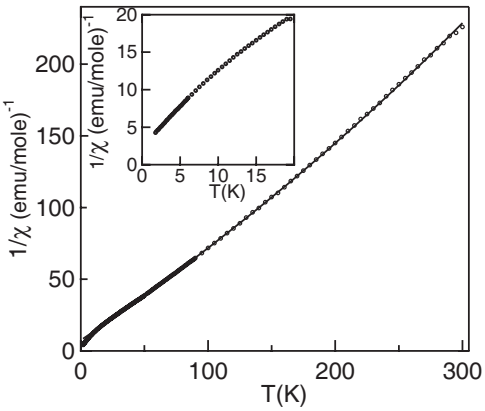

FIG. 3. Temperature dependence of the inverse of the magnetic susceptibility χ^{-1} of $YbRh_2Pb$ measured in a field of 1000 Oe. The solid line is a fit to a modified Curie–Weiss law at 50 K$<T<$300 K (see text). The inset shows $1/\chi$ below $T=20$ K.

resistivity is derived from the electron-phonon interaction and, furthermore, that the Debye temperature in $YbRh_2Pb$ is unusually small. However, we will later show by using the heat capacity data that the Debye temperature in $YbRh_2Pb$ is ~213 K. It is notable as well that the resistivity does not saturate at high temperatures, suggesting that the electronic mean free path is still much larger than the lattice constant at room temperature. We cannot entirely rule out the possibility that the fundamental electronic excitations themselves are anomalous, as was found in the normal state of the high temperature oxide superconductors.[14]

The magnetic properties of $YbRh_2Pb$ establish that the Yb^{3+} moments are well localized. The temperature dependence of the dc magnetic susceptibility $\chi(T)$ was measured in a field of 1000 Oe, as shown in Fig. 3. The magnetic susceptibility above 50 K is well described by a modified Curie–Weiss law ($\chi=\chi_0+C/(T-\Theta)$), which yields $\chi_0=-0.001$ emu/mole Yb, a Weiss temperature $\Theta=-12.4\pm0.1$ K, and an effective magnetic moment $\mu_{\text{eff}}=3.66\pm0.04\mu_B$ per Yb ion, a substantial fraction of the value of $4.54\mu_B$ expected for a free Yb^{3+} ion. The inset of Fig. 3 shows that $1/\chi$ deviates below the linear behavior at $T<20$ K but remains finite at the lowest temperatures. We will argue below that the general lack of agreement between the measured susceptibility and a single Curie–Weiss expression at low temperatures results from significant CEF effects, yielding a highly temperature dependent effective moment in $YbRh_2Pb$.

We derived the basic ingredients for devising a crystal field scheme for $YbRh_2Pb$ from heat capacity measurements. The temperature dependence of the heat capacity $C(T)$ measured in zero field and at temperatures as large as 70 K is shown in Fig. 4(a). We have estimated the phonon contribution to the heat capacity C_{ph} by fitting the high temperature $C(T)$ to the Debye expression with only the varied parameter θ_D (the Debye temperature). A good fit was obtained for $\theta_D=213\pm5$ K. C_{ph} is subtracted from $C(T)$ in Fig. 4(a) to isolate the remaining magnetic and electronic contributions to the heat capacity. The latter is expected to result in a component of the heat capacity, which is linear in temperature, $C_{\text{el}}=\gamma T$. Accordingly, we have plotted C/T as a func-

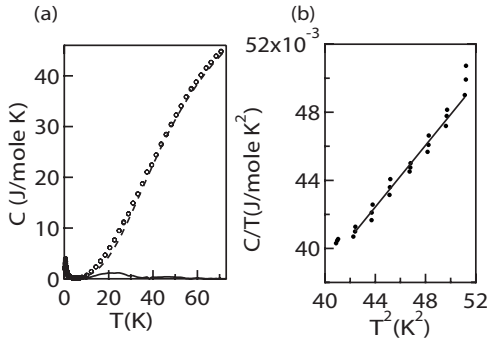

FIG. 4. (a) Temperature dependence of the heat capacity C (○) of $YbRh_2Pb$ measured in zero field. The dashed line represents the Debye heat capacity and the solid line is the heat capacity with the lattice contribution subtracted. (b) The electronic part of the heat capacity $C_{el}=\gamma T$ is determined from this plot of $C/T=\gamma+\beta T^2$.

tion of T^2 in Fig. 4(b), demonstrating that the electronic contribution can at best be identified over a very limited range of temperatures, yielding $\gamma=4\pm1$ mJ/mole K^2. We conclude that the purely electronic contribution to the heat capacity is very small, as would be expected for weakly correlated conduction electrons or alternatively for a low density of conduction electrons for $YbRh_2Pb$. This implies, in turn, that $C-C_{ph}$ is largely magnetic. An expanded view of the temperature dependence of $C-C_{ph}$ is presented in Fig. 5, which is accompanied by the associated entropy S. The sudden increase in $C-C_{ph}$ near 0.57 K indicates a magnetic phase transition, which is possibly superposed on a broad Schottky peak. We have approximated $C-C_{ph}$ to zero temperature to account for the part of the heat capacity below 0.35 K, which was inaccessible in our measurement. The entropy difference associated with the magnetic phase transition is only $0.78R$ ln 2, indicating that magnetic order does not develop from a well defined doublet ground state; alternatively, an onset of the weak Kondo effect with the Kondo temperature $T_K<0.5$ K can account for a reduced entropy. The entropy is roughly constant between 2 and 10 K, subsequently increasing in proximity to a large Schottky anomaly centered at 28 K and approaching the full R ln 2 only near 30 K.

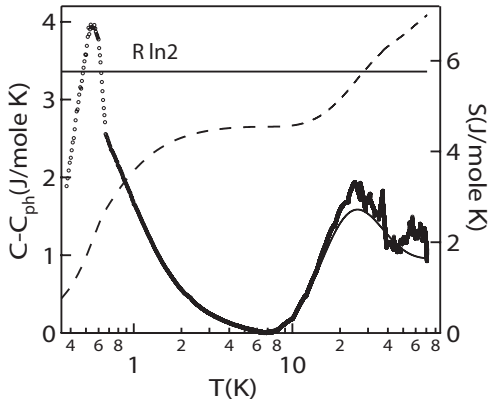

FIG. 5. Temperature dependence of the nonphonon heat capacity $C-C_{ph}$ (○) and the entropy S (dashed line) of $YbRh_2Pb$ measured in zero field. The peak in $C-C_{ph}$ centered at 28 K is well fit by the Schottky expression described in the text (solid line).

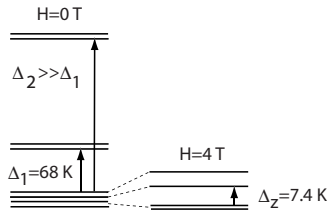

FIG. 6. Proposed zero field CEF scheme for Yb^{3+} in $YbRh_2Pb$ (left). Application of a magnetic field lifts the degeneracy of the ground state quartet by an amount Δ_z, which is 7.4 K at 4 T (right).

Although the site symmetry of Yb in $YbRh_2Pb$ is tetragonal and, hence, the CEF scheme must consist of four doublets, we show that the first excited doublet lies sufficiently close to the ground state doublet and that the ground state can be considered a quartet. In Fig. 6, we schematically illustrate the CEF splitting scheme in $YbRh_2Pb$, which is derived from our heat capacity measurements. The best fit to the broad maximum in the heat capacity at ~28 K (Fig. 5) was obtained by assuming a fourfold degenerate ground state separated by an energy of $\Delta_1=68\pm5$ K from the first excited state, which is a doublet. The second excited doublet is separated by $\Delta_2\gg\Delta_1$. We conclude that the full Yb moment can only be regained at temperatures much higher than 68 K, and that at lower temperatures, there is a substantially smaller and temperature dependent effective Yb moment.

To further test this CEF scheme, we have measured $C(T)$ in a variety of fields between 0 and 4 T. The data are presented in Fig. 7. Magnetic fields suppress the heat capacity jump at the magnetic transition. The ordering temperature, which is determined from the local maximum on $C(T)$ also decreases in field, and Fig. 8 indicates that a magnetic field >4 T is required to completely suppress magnetic order. For fields greater than ~2 T, the measured heat capacity mostly consists of a single broad peak, which shifts to higher temperatures with increasing magnetic field. We attribute this peak to the Zeeman splitting of the ground state of $YbRh_2Pb$, which is a quartet in zero field. The field dependence of the heat capacity represented in Fig. 7 can be understood by assuming that the quartet is Zeeman split by the field into a

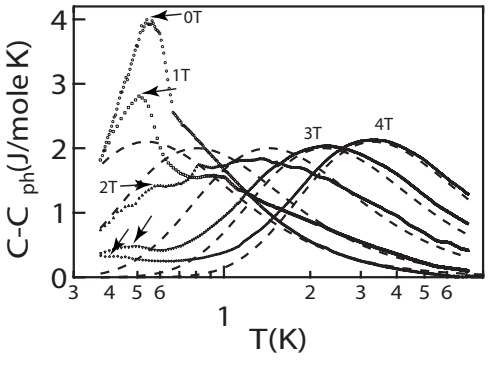

FIG. 7. Temperature dependence of the heat capacity of $YbRh_2Pb$ measured in magnetic fields with the lattice contribution subtracted. The dashed lines represent the Schottky heat capacity C_{Sch} of the two-level system, when the levels are split by the magnetic field.

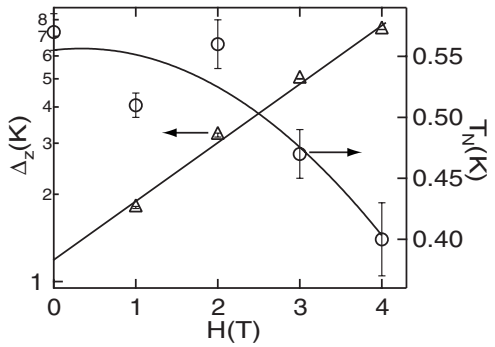

FIG. 8. Suppression of the magnetic ordering temperature T_N with increasing magnetic field (○); △ indicates the Zeeman splitting Δ_z of the ground state quartet, which is taken from the Schottky analysis of the heat capacity described in the text. The solid lines are guides for the eye.

ground state doublet and two excited singlets, as depicted in Fig. 6. Accordingly, in a field of 4 T, the heat capacity reaches ~2 J/mole K at $T_{max}=0.448\Delta_z=3.3$ K as expected of a system with thermally activated occupation levels and with a degeneracy ratio of 0.5.[15] The splitting Δ_z between the ground doublet and first excited doublet is deduced from Schottky fits to the data of Fig. 7, and Δ_z itself is plotted in Fig. 8. We note that including a second excited singlet state to this analysis did not significantly improve the quality of the fits. Δ_z approximately linearly increases to a value of 7 K in a field of 4 T. Interestingly, Fig. 8 suggests that there is a residual splitting of ~1.5 K in the zero field, which may perhaps account for the broad peak on which the magnetic anomaly is superposed (Fig. 5). Apart from this small splitting, the evolution of the heat capacity with magnetic fields indicates that the zero field ground state of $YbRh_2Pb$ is fourfold degenerate. It would be interesting to further test this level scheme in $YbRh_2Pb$ by using inelastic neutron scattering experiments.

Given the magnitudes of the splittings in the CEF scheme of $YbRh_2Pb$ that are revealed by our analysis of the heat capacity, we expect that the effective Yb moment considerably varies over the temperature range of 1.8–70 K spanned by our measurements. As we have observed in our discussion of Fig. 3, this implies that χ cannot be fitted by the Curie-Weiss law over an extensive range of temperatures. This is illustrated in the Fig. 9, where we plotted the effective magnetic moment $\mu_{\text{eff}}(T)=\sqrt{\frac{3k_BT\chi}{N}}$ as a function of temperature.

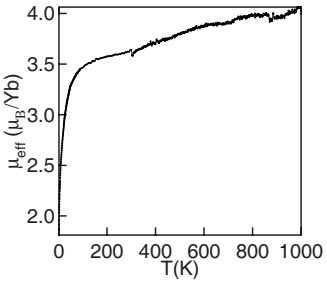

FIG. 9. The temperature dependent effective magnetic moment $\mu_{\text{eff}}(T)=\sqrt{\frac{3k_BT\chi}{N}}$ vs T.

The data at $300<T<1000$ K were obtained by using the VSM. With increased temperature, μ_{eff} increases as the excited states become occupied. The full Yb^{3+} Hund's rule moment of $4.54\mu_B$ is only regained at temperatures in excess of 1000 K.

The interplay between moment degeneracy and intermoment interactions strongly impacts the stability of magnetic order in $YbRh_2Pb$, which only occurs below 0.57 K. While neutron diffraction measurements are required to unambiguously establish the type of magnetic order, the relatively weak field dependence of the transition temperature and the absence of appreciable broadening of the transition in the heat capacity suggest that $YbRh_2Pb$ is an antiferromagnet. Magnetic order arises within a ground state quartet, which is further split into a doublet separated from the first of two excited singlets by ~1.5 K. Increasing this separation Δ_z with magnetic field results in the further suppression of the ordering temperature T_N. We observe that the successive actions of tetragonal and uniaxial CEF effects result in a paramagnetic state with a moment much reduced from the free ion value. At the same time, the small residual resistivity and the small electronic heat capacity suggest extremely weak hybridization between the Yb moment and the conduction electrons, and subsequently, a small RKKY interaction among Yb moments. For these reasons, we believe that the magnetic order in $YbRh_2Pb$ is driven by a vanishingly small RKKY interaction acting on moments that have been reduced to a minimal value by CEF splittings which, while small in an absolute sense, are very large compared to T_N itself.

IV. CONCLUSION

We have synthesized the intermetallic Heusler compound $YbRh_2Pb$, which magnetically orders below $T_N=0.57$ K. The electrical resistivity displays an unusual linear temperature dependence, and its small residual value is consistent with a good crystalline quality. Analyses of the heat capacity and the magnetic susceptibility indicate that the CEF splits the eightfold degenerate ground state of Yb^{3+} into a ground state quartet and two excited doublets separated from the ground state by $\Delta_1=68$ K and $\Delta_2\sim1000$ K, respectively. Magnetic fields further split the ground state, and we propose that this reduction in the effective moment is responsible for the observed reduction in the ordering temperature. Given the strong current interest in the quantum critical behavior that is found near phase transitions that occur at zero or low temperatures,[16] it is interesting to consider whether $YbRh_2Pb$ belongs to this class of materials. While $YbRh_2Pb$ orders at a very low temperature, one which can be reduced further by applying a magnetic field, it is unlikely that quantum critical behavior will be observable in this system. The purely local moment nature of the magnetism, paired with the absence of correlation effects among the conduction electrons, suggest that $YbRh_2Pb$ belongs instead to the weak coupling limit of the Doniach phase diagram.[17] Without a large magnetic energy scale, the conventional critical phenomena associated with the small but finite temperature magnetic phase transition will limit any non-Fermi liquid behavior in $YbRh_2Pb$ to very small reduced temperatures.[18]

ACKNOWLEDGMENTS

Work at the University of Michigan was performed under NSF Grant No. DMR-0405961. D.A.S. acknowledges useful conversations with Z. Fisk. The electron microprobe used in this study was partially funded by Grant No. EAR-99-11352 from the National Science Foundation. The use of the National Synchrotron Light Source, Brookhaven National Laboratory, was supported by the U.S. Department of Energy, Office of Science, Office of Basic Energy Sciences, under Contract No. DE-AC02-98CH10886. We are grateful to Joseph Lauher for the use of x-ray diffraction facilities at the Stony Brook University Chemistry Department.

*fermiliquid@gmail.com

[1] P. J. Webster, Contemp. Phys. **10**, 559 (1969).
[2] M. Ishikawa, J.-L. Jorda, and A. Junod, in *Superconductivity in d- and f-Band Metals*, edited by W. Buckel and W. Weber (Kernforschungszentrum, Karlsruhe, 1982), p. 141.
[3] S. K. Malik, A. M. Umarji, and G. K. Shenoy, Phys. Rev. B **31**, 6971 (1985).
[4] H. A. Kierstead, B. D. Dunlap, S. K. Malik, A. M. Umarji, and G. K. Shenoy, Phys. Rev. B **32**, 135 (1985).
[5] R. N. Shelton, L. S. Hausermann-Berg, M. J. Johnson, P. Klavins, and H. D. Yang, Phys. Rev. B **34**, 199 (1986).
[6] H. B. Stanley, J. W. Lynn, R. N. Shelton, and P. Klavins, J. Appl. Phys. **61**, 3371 (1987).
[7] W.-H. Li, J. W. Lynn, H. B. Stanley, T. J. Udovic, R. N. Shelton, and P. Klavins, Phys. Rev. B **39**, 4119 (1989).
[8] C. L. Seaman, N. R. Dilley, M. C. de Andrade, J. Herrmann, M. B. Maple, and Z. Fisk, Phys. Rev. B **53**, 2651 (1996).
[9] Y.Aoki, H. R. Sato, H. Sugawara, and H. Sato, Physica C **333**, 187 (2000).
[10] K. Gofryk, D. Kaczorowski, T. Plackowski, A. Leithe-Jasper, and Yu. Grin, Phys. Rev. B **72**, 094409 (2005).
[11] J. C. Suits, Solid State Commun. **18**, 423 (1976).
[12] TOPAS V3: General Profile and Structure Analysis Software for Powder Diffraction Data, Bruker AXS, Karlsruhe, Germany. An academic version of TOPAS is available from (http://members.optusnet.com.au/).
[13] M. F. Gendron and R. E. Jones, J. Phys. Chem. Solids **23**, 405 (1962).
[14] See, for instance, L. Civale and E. N. Martinez, Phys. Rev. B **38**, 928 (1988), and the references therein.
[15] J. G. Sereni, in *Handbook on the Physics and Chemistry of Rare Earths*, edited by K. A. Gschneidner, Jr. and L. Eyring (North-Holland, Amsterdam, 1991), p. 141.
[16] G. R. Stewart, Rev. Mod. Phys. **73**, 797 (2001).
[17] S. Doniach, Physica B & C **91**, 231 (1977).
[18] A. J. Millis, Phys. Rev. B **48**, 7183 (1993).